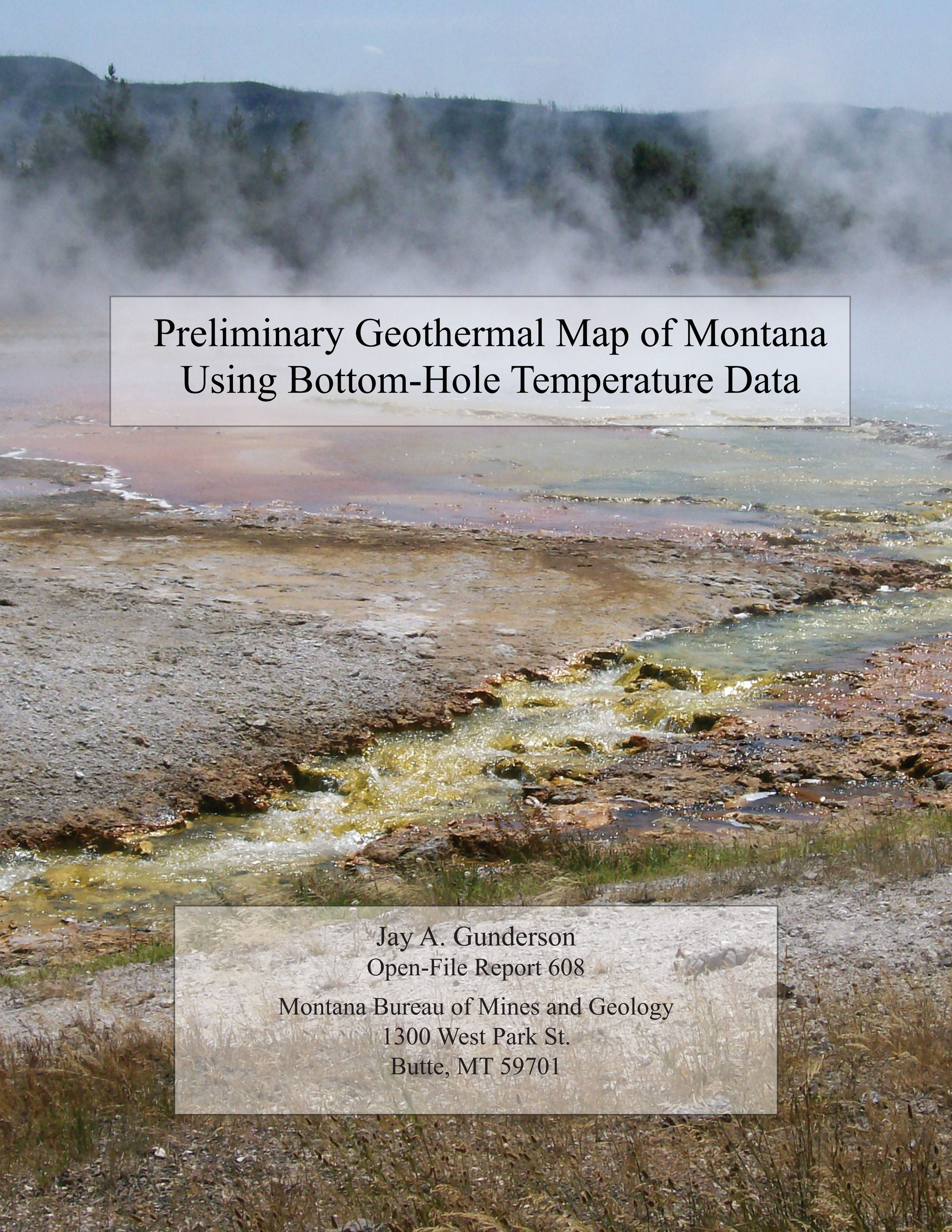

Preliminary Geothermal Map of Montana Using Bottom-Hole Temperature Data

Jay A. Gunderson

Open-File Report 608

Montana Bureau of Mines and Geology
1300 West Park St.
Butte, MT 59701

Introduction

Heat from the decay of radioactive isotopes in the earth's mantle and crust radiates from the earth's interior and provides an enormous source of geothermal energy that could be captured and utilized. Because temperature generally increases with depth, groundwater in the subsurface is heated as it migrates downward through rock layers. Naturally occurring hot water and steam, whether shallow or deep, can be produced to the surface and used in heat exchangers or steam turbines to generate electrical power. The U.S. Geological Survey (USGS) estimates that within the western U.S., over 9,000 Megawatts-electric (MWe) of electrical power generation potential exists from known geothermal systems, with another 30,000 MWe likely from undiscovered resources (Williams and others, 2008).

As with many other forms of renewable energy, geothermal resources have not been aggressively explored or exploited because of the availability of cheap, accessible fossil fuels. Only geothermal sites with near-surface hot water or steam that can be used directly in steam turbines (e.g., The Geysers geothermal complex in California) have attracted interest because they are able to compete economically with traditional energy sources. Recently, however, more opportunities have emerged for the use of low- (<190ºF) and moderate-temperature (190ºF–300ºF) geothermal resources in Organic Rankine Cycle systems that utilize fluids with lower boiling points to drive power-generating turbines. Also, in the future, Enhanced Geothermal Systems could be engineered so that water is circulated into the subsurface, along permeable conduits within the rocks to absorb heat, and back to the surface for re-use. Because low to moderate temperatures may be suitable for these or other geothermal applications, it is necessary to identify regions with suitable thermal characteristics.

Bottom-hole temperatures (BHT) from well logs are one source of data that can be easily gathered and analyzed to identify potential geothermal "hot spots." In the early 1970s, researchers of the AAPG Geothermal Survey of North America project collected BHT data from more than 10,000 wells in the U.S., Mexico, and Canada. Most of these U.S. wells occur along a band that stretches from the Gulf Coast of Texas and Louisiana northwestward along the Rocky Mountain Front to Montana—i.e., the primary petroleum-producing areas of the continental U.S. Based on these BHT data, a geothermal gradient map for North America was published by DeFord and Kehle (1976).

More recently, Blackwell and Richards (2004b) used the AAPG and other data to construct their Geothermal Map of North America depicting regional heat flow. Similar maps have been published by the Idaho National Engineering and Environmental Laboratory (Brizzee and Laney, 2003), the National Renewable Energy Laboratory (Roberts, 2009), and the Montana Bureau of Mines and Geology (Sonderegger and others, 1981), among others. All show a large area of "geothermal potential" in eastern Montana roughly coincident with the extent of the Fort Union Formation, but lack the detail necessary to identify specific low- to moderate-temperature geothermal anomalies. The objective of this study is to compile additional BHT data for Montana, and use these data to provide a more detailed assessment of temperature and geothermal gradient variations across the State.

Methods

Over 40,000 petroleum exploration wells have been drilled in Montana (fig. 1). Bottom-hole temperature data were gathered from wireline log headers for nearly 9,500 oil and gas wells as part of this study. Preference was given to deep wells (>3,000 ft) with higher temperatures because they provide better averaging of vertical temperature gradients and to avoid potential confusion with ambient temperatures. For each well where multiple log runs were conducted, we chose the maximum recorded BHT. Deviated and horizontal wells were used only where directional surveys could be located to obtain true vertical depth. The remaining nearly 30,000 wells were excluded because they either have no digital log data available (~12,000), have no BHT values reported on the log headers (~3,000), or are shallow gas wells drilled into existing fields where nearby wells are already included (~15,000). The high-density spacing of shallow gas wells in north-central Montana can be seen in figure 1.

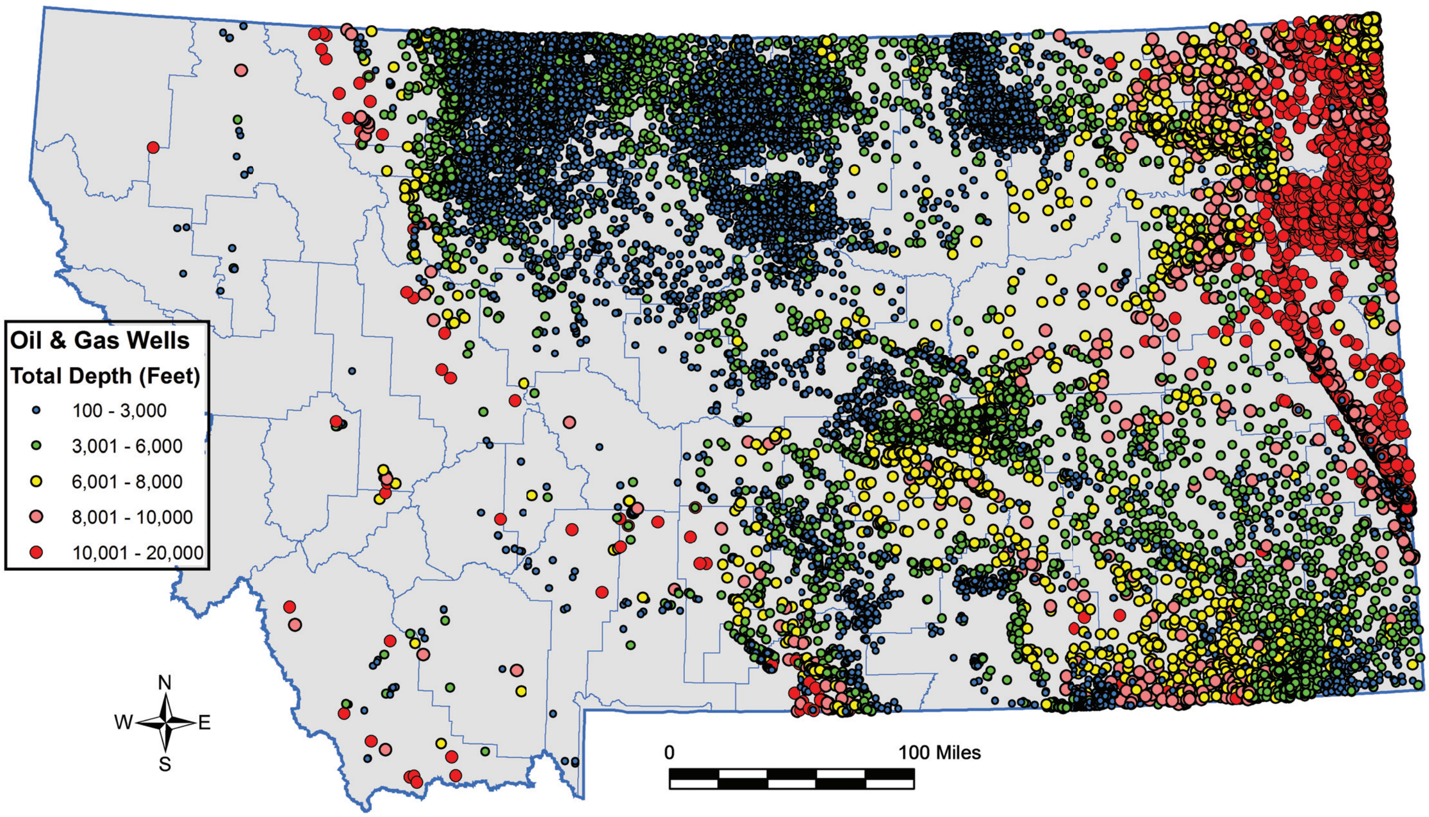

Figure 1. Distribution of petroleum exploration wells in Montana showing the total vertical depth drilled. Deeper drilling is concentrated in the Williston Basin of Eastern Montana. Shallow wells dominate north-central Montana.

The 1,013 AAPG data points for Montana were not used because they do not include a unique identifier such as API number and therefore could not be easily verified for accuracy. However, a simple comparison of BHT values by location suggests that nearly all of the AAPG data deeper than 3,000 ft are also present in our dataset. We included 400 additional points from the AAPG dataset for neighboring states (ND, SD, WY) and Canadian provinces (AB, SK) to provide mapping control and continuity across state borders.

BHT data are inherently inaccurate because borehole temperatures are obtained from drilling fluid samples rather than directly from the formation, and because they are almost always measured under transient thermal conditions. During drilling, the drilling fluid (or mud) is circulated in the wellbore where it continuously contacts and cools the geologic formations exposed in the borehole. This can lower the formation temperature tens of degrees Fahrenheit. Conversely, heat from the formation is transferred to the drilling mud, and although temperature measurements are taken after some period of "stopped circulation," it is rarely long enough for the formation and mud to have reached thermal equilibrium. Thus, measured mud temperatures are nearly always lower than the formation temperatures they are assumed to represent. Nevertheless, due to lack of better quality data, BHTs can be used to constrain the subsurface thermal regime and regional temperature gradients.

To address the "non-equilibrium" issue, Harrison and others (1983) compared raw AAPG BHT data for Oklahoma with corresponding equilibrium temperatures (mostly from drill-stem tests) and developed a graphical solution to correct raw BHT data. Blackwell and Richards (2004a) fit a line to that graphical representation to derive the so-called "Harrison correction" equation (1):

$$Tc = -16.51213476 + 0.01826842109 * Z - 2.344936959 \times 10^{-6} * Z^{2}, \qquad (1)$$

where Z is depth in meters and Tc is the temperature correction in degrees Celsius. The equation has been widely used by subsequent workers, including Blackwell and Richards (2004b) in developing their heat flow maps. We applied this first-order correction to the BHT measurements for Montana to obtain corrected temperatures (fig. 2). The crossplots in figure 3 show raw and corrected temperature data versus depth. The raw data show a subtle break around 3,500 ft, where shallower wells have elevated temperatures with respect to the overall trend. After applying the correction, the temperature data more closely follow a single trend.

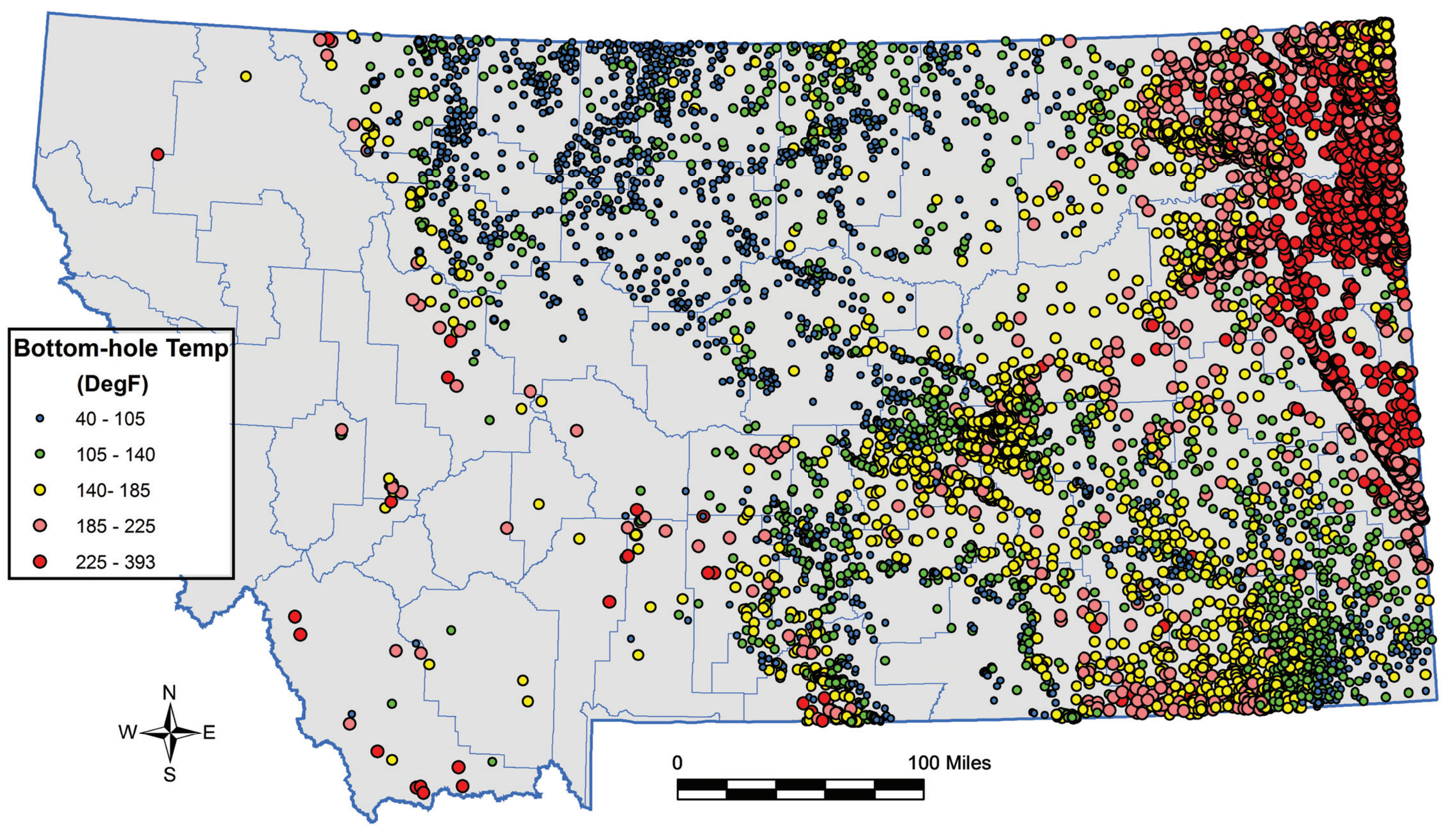

Figure 2. Corrected bottom-hole temperatures from 9,500 petroleum exploration wells. Temperature is closely correlated to drilled depth (see fig. 1). Temperatures above 225°F are common in deep wells of the Williston Basin.

The temperature map shown in figure 2 can be readily used to identify specific oil and gas wells and/or fields with temperatures above 200ºF that may be candidates for using co-produced fluids in an Organic Rankine Cycle generator. However, other local hot spots can be easily overlooked simply because some wells are not drilled very deep and have correspondingly low temperatures. Direct comparison of temperatures to identify geothermal anomalies is not particularly effective when drilling depths vary by more than about 1,000 ft.

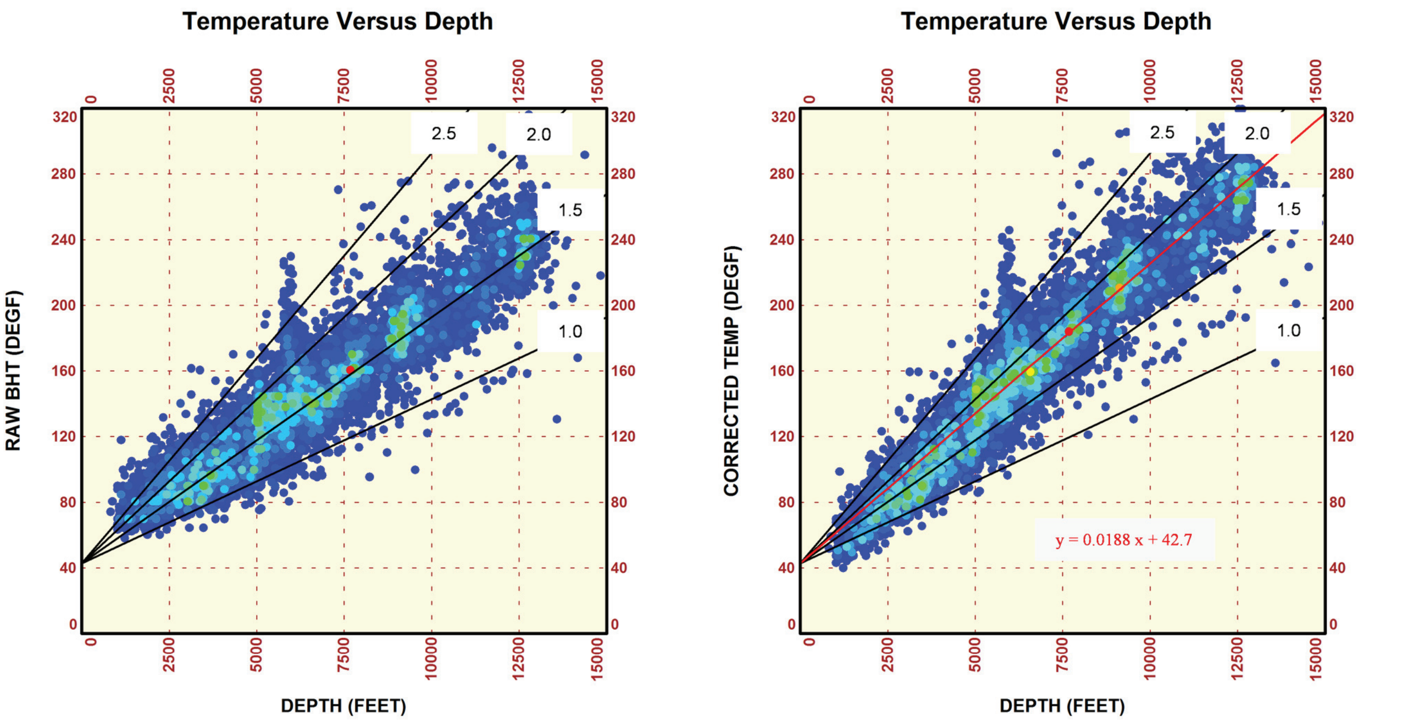

Figure 3. Crossplots of bottom-hole temperature versus depth for: (a) raw temperature measurements, and (b) corrected temperatures using the Harrison (1983) correction. Colors represent frequency, with warmer colors (green/yellow) indicating higher data frequency. Lines of constant geothermal gradient (ºF/100 ft) are shown in black for reference. The red regression line in (b) is the average geothermal gradient of 1.88ºF/100 ft.

For spatial comparison, temperatures were "normalized" by computing geothermal gradient (i.e., the rate of temperature change with depth) using equation 2.

$$\text{Geothermal Gradient} = [(\text{BHT} - \text{MST}) / \text{Depth}] * 100, \qquad (2)$$

where MST is the mean annual surface temperature, taken to be 42.7ºF for Montana (http://coolweather.net/statetemperature/montana_temperature.htm). In equation 2, BHT and MST are in degrees Fahrenheit, depth is in feet, and geothermal gradient is reported in degrees Fahrenheit per 100 ft. Geothermal gradients are shown in figure 4. Anomalously high gradients indicate that elevated temperatures are likely to be encountered at depth, but do not necessarily correlate with the highest measured temperatures (compare to fig. 2). Finally, the gradient data were gridded using ESRI's ArcGIS software and applying an inverse distance weighting algorithm with a 3,000 meter cell size (fig. 5).

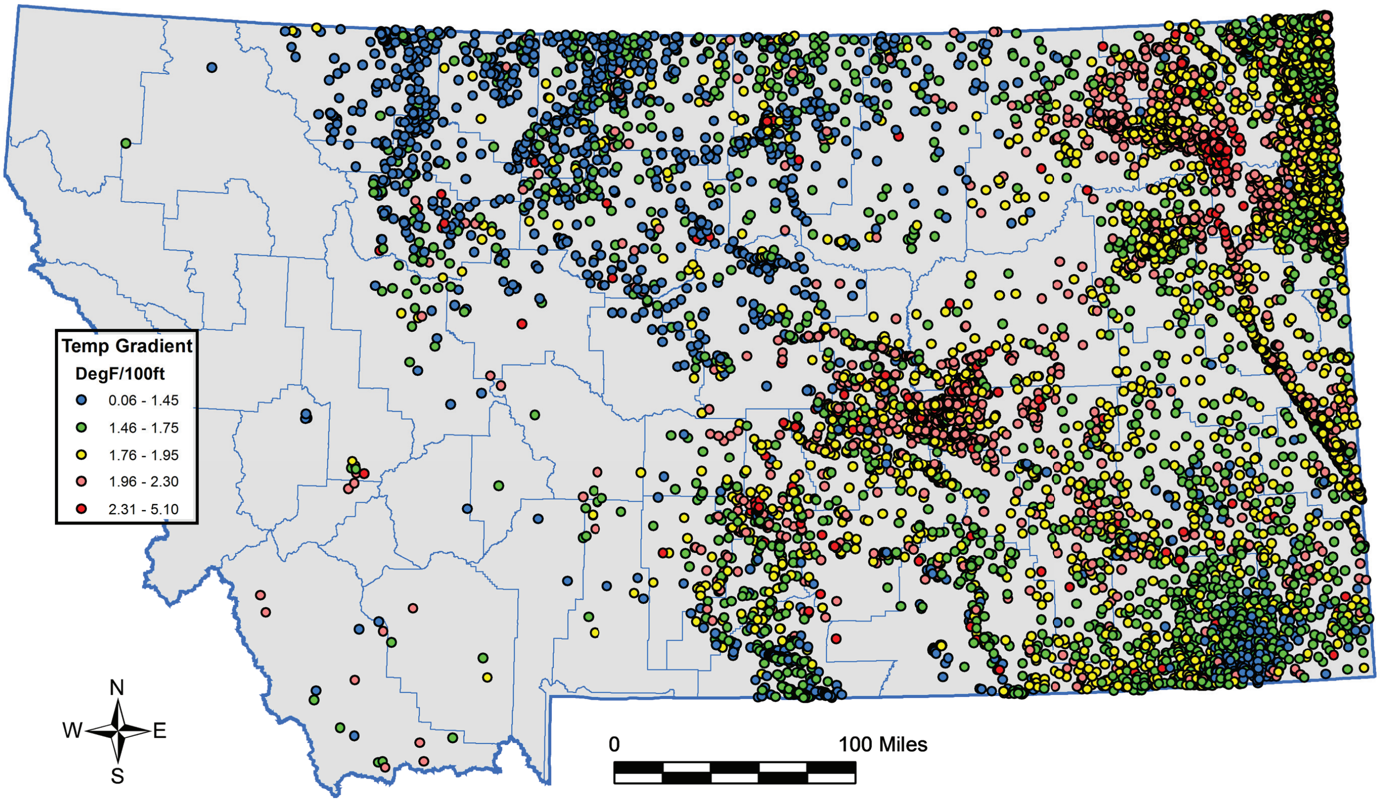

Figure 4. Temperature gradient in degrees Fahrenheit per 100 feet (ºF/100ft).

Results

Bottom-hole temperature data for approximately 9,500 oil and gas wells were compiled. These data constitute a new geothermal dataset that provides, at a minimum:

1) A direct indicator of existing petroleum wells with water that is hot enough to be considered for power generation using co-produced fluids.

2) The ability to map and study geothermal gradients to illuminate hot spots on a more detailed basis than has been done previously.

As expected, the spatial distribution of temperature data is closely related to drilled depth. A simple linear regression of temperature versus depth gives an average, or regional, geothermal gradient of about 1.9ºF/100 ft (fig. 3). Temperatures greater than about 190ºF, shown in orange and red in figure 2, are prevalent in much of the Williston Basin and south along the Cedar Creek Anticline (refer to fig. 5 for structural elements). Several existing oil fields in this region are likely to have very good potential for co-production of hot water that could be used in binary-cycle power generation. Most of the wells in these fields are 10,000–15,000 ft deep.

The geothermal gradient data shown in figure 4 vary considerably even over relatively short distances. Much of the apparent "noise" is simply an artifact of our narrowly banded color scale, and could be eliminated if we applied a broader scale similar to Blackwell and Richards (2004a). In other cases, noise can be attributed to inaccuracies in BHT measurements made under transient conditions. Shallow wells (<3,000 ft deep) are particularly unreliable. At shallow depths, small temperature errors are magnified to give significant errors in temperature gradient. Table 1 illustrates the impact that a ±10ºF temperature error has on temperature gradient at several different depths. The effect can also be easily visualized by examining the convergence of gradient lines at shallow depths on the crossplots in figure 3.

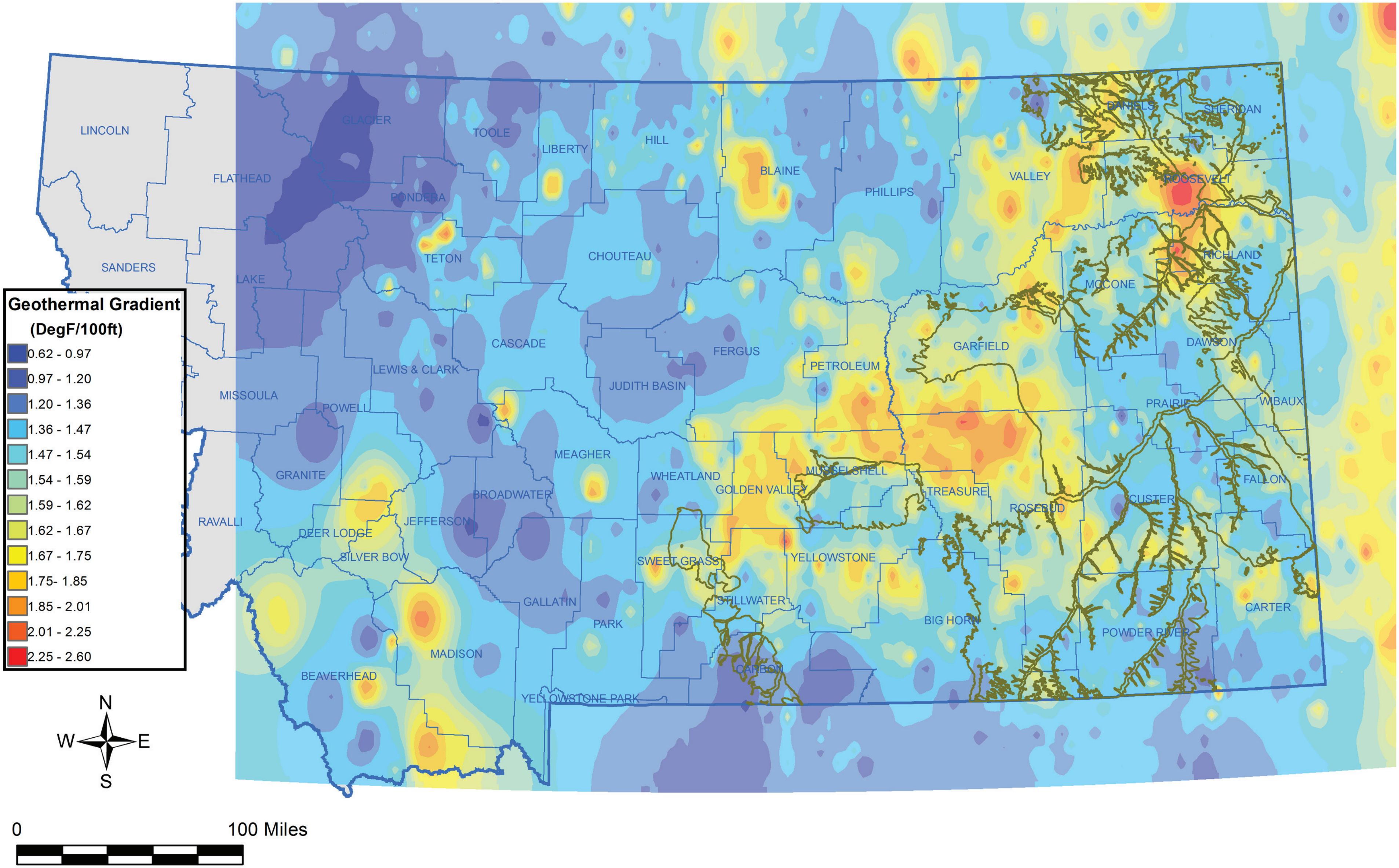

Figure 5. Preliminary contour map of geothermal gradient. The extent of the Fort Union Formation in eastern Montana is outlined in olive green for reference, as a convenient way to show that the higher geothermal gradients tend to occur in structurally complex areas between basins.

Table 1. Error analysis showing the impact of temperature errors on geothermal gradient at various depths.

(a)	(b)	(c)	(d)	(e)		(f)
DEPTH (ft)	TGRAD (ºF/100 ft)	TEMP (ºF)	TEMP (ºF)	TGRAD (ºF/100 ft)		% ERROR
2000	1.90	81	±10	1.40–2.40		±26%
5000	1.90	138	±10	1.70–2.10		±10%
8000	1.90	195	±10	1.78–2.02		±6%
15000	1.90	328	±10	1.83–1.97		±4%

Note. Columns are: (a) depth, (b) assumed temperature gradient, (c) estimated temperature based on depth and temperature gradient (columns a and b), (d) hypothetical error in BHT, (e) corresponding range in temperature gradients given a ±10 error in BHT, and (f) percent error in temperature gradient.

Figure 5 is a preliminary contour map of geothermal gradient for Montana that can be used to identify geothermal trends and anomalies. It is similar in appearance to Blackwell and Richards' (2004b) heat flow map on a regional scale, but provides much greater detail.

In central and eastern Montana, a large region of elevated temperature gradient extends from northeast to southwest and roughly coincides with the area of "geothermal potential" shown on many other published maps (e.g., Blackwell and Richards, 2004b; Brizzee and Laney, 2003; Roberts, 2009; Sonderegger and others, 1981). However, local variations are more complex than have been depicted in previous maps. High geothermal gradients do not merely coincide with the Fort Union Formation sedimentary cover, but appear to correlate with structural trends and specific structural features (refer to fig. 6). These include not only the well-known geothermal anomaly at Poplar Dome, but also those occurring along the Cat Creek Lineament from the Big Snowy Uplift to Porcupine Dome and to some extent along the Lake Basin Lineament.

In western Montana, west of the Rocky Mountain Front, the map is based on only a few data points because of the limited oil and gas exploration in that part of the State, and geothermal anomalies should be considered very preliminary until more data can be included.

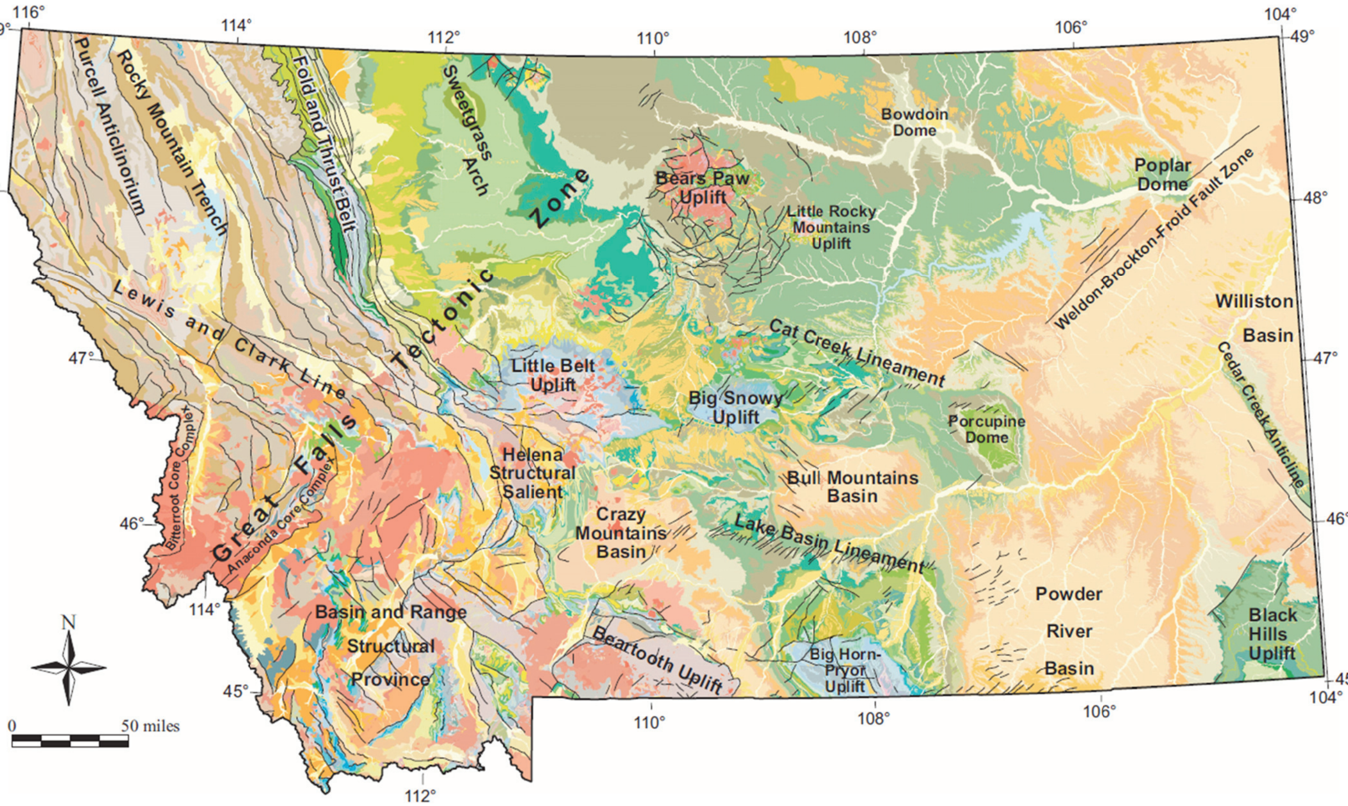

Figure 6. Major tectonic features of Montana (from Vuke and others, 2007). In the eastern half of Montana, the Tertiary Fort Union Formation is shown in tan/brown colors, with older Cretaceous rocks in green tones.

Summary

Analysis of temperature data recorded in petroleum wells provides information on regional geothermal hot spots, and helps identify specific oil wells and fields that could be suitable as a geothermal energy source for driving electric generators.

The geothermal gradient map for Montana provides more detail than previous maps and suggests that areas of high heat flow in central and eastern Montana may be related to structural elements—structural highs in particular—rather than thick sedimentary cover.

The geothermal map is preliminary and will be updated as additional information becomes available. Continued efforts to add high-quality data to the geothermal database for Montana will include additional BHT data and temperature logs acquired in boreholes.

Further analyses will need to address the following issues:

1) Verify the reliability of shallow data;
2) Where data are sufficient and reliable, assess whether our understanding of geothermal gradients can be improved by segregating data vertically (e.g., by formation or depth); and
3) Confirm the appropriateness of the Harrison (1983) correction for BHT data from Montana, or consider alternatives.

References

AAPG, American Association of Petroleum Geologists, CSDE, COSUNA, and Geothermal Survey Data CD-ROM, 1994.

Blackwell, D.D., and Richards, M., 2004a, Calibration of the American Association of Petroleum Geologists geothermal survey of North America BHT data base, prepared for the American Association of Petroleum Geologists annual meeting, Dallas, TX: Poster session Paper No. 87616.

Blackwell, D.D., and Richards, M. 2004b, Geothermal map of North America: American Association of Petroleum Geologists, scale 1:6,500,000.

Brizzee, J., and Laney, P., 2003, Montana geothermal resources, prepared for the United States Department of Energy Office of Energy Efficiency and Renewable Energy Geothermal Technologies Program Publication No. INEEL/MIS-2002-119, Rev.1, scale 1:1,000,000.

DeFord, R.K., and Kehle, R.O., 1976, Geothermal gradient map of North America: American Association of Petroleum Geologist and U.S. Geological Survey, scale 1:5,000,000.

Harrison, E.W., Luza, K.V., Cheung, P.K.., and Prater, M.L., 1983, Geothermal resource assessment in Oklahoma: Oklahoma Geological Society Special Publication 83-1.

Montana Annual Temperature and Records, Retrieved February 2, 2011. From http://coolweather.net/statetemperature/montana_temperature.htm.

Roberts, B.J., 2009, Geothermal resource of the United States: Locations of identified hydrothermal sites and favorability of deep enhanced geothermal systems (EGS), National Renewable Energy Laboratory. Retrieved February 8, 2011, from http://www.nrel.gov/gis/images/geothermal_resource2009-final.jpg.

Sonderegger, J.L., Bergantino, R.N., and Kovacich, S., 1981, Geothermal resources map of Montana and corresponding tables: Montana Bureau of Mines and Geology Hydrogeologic Map 4, scale 1:1,000,000.

Vuke, S.M., Porter, K.W., Lonn, J.D., and Lopez, D.A., 2007, Geologic map of Montana, Montana Bureau of Mines and Geology Geologic Map 62.

Williams, C.F., Reed, M.J., Mariner, R.H., DeAngelo, J., and Galnis, S.P., 2008, Assessment of moderate- and high-temperature geothermal resources of the United States, in Hendley, J.W., ed., U.S. Geological Survey Fact Sheet 2008-3082. Retrieved December 15, 2010, from http://pubs.usgs.gov/fs/2008/3082/pdf/fs2008-3082.pdf.